ORIGINAL RESEARCH PAPER

Optimization of process variables by response surface methodology for methylene blue dye removal using Spruce sawdust/MgO nano-biocomposite

Seyed Hassan Sharifi*, Hassan Shoja

Wood and Paper Science Department, Faculty of Natural Resources, Sari Agricultural Sciences and Natural Resource University, Sari, Iran

ABSTRACT

The purpose of this investigation is to study the influence of Spruce sawdust (SD) coated by magnesium oxide (MgO) nanoparticles in the removing of methylene blue (MB) from an aqueous solution which is in a batch system. The adsorbent was characterized by FTIR, FE-SEM, BET and XRD analysis. The high adsorption potential of SD-MgO nano-biocomposite was revealed by these findings, therefore, it is usable for dye-containing wastewater treatment. By investigating the impact of particular conditions like MB concentrations, the dose of adsorbent and pH, it became possible to confirm the effectiveness of the process. The OOP (which stands for Optimum Operating Parameters) were evaluated by RSM (which stands for Response Surface Methodology) which is based on BBD (Box-Behnken design) and is used for removing MB dye. The adsorbent dosage is the highest effective degree of the individual factor on MB removal. Maximum removal of MB dye was detected at pH 11 with 3.50 g L^{-1} adsorbent dosage. The surface area of 0.873 m^2 g^{-1} and mesoporous adsorbent prepared gave good adsorption capacity of 26.657 mg g^{-1} for MB. Furthermore, in order to predict the empirical variables' significance, the variances' analysis (ANOVA) was used. The predicated removal efficiency which is proved to be the potency of the process and its effectiveness was found to be 94.05%. Different equilibrium and kinetic models were utilized to the experimental data. Both Pseudo-second order kinetic model and Freundlich adsorption isotherm showed the better fitness to the experimental data.

Keywords: *Adsorption; Box-Behnken Design; Dye; Mgo Nanoparticles; Nano-Biocomposites*

INTRODUCTION

Industrial activities cause wastewater in large volume including hazardous inorganic (metals) or organic (microbes, dyes/ pigments) species. One of the visual remarkable pollution which is generated from paper and pulp, plastic, cosmetic, distilleries, textile and tanneries industries is dye contaminated wastewater [1]. Dyes play a role as a main raw material in different kind of industries. However,

their disposal in water bodies exhibits an adverse effect on the aquatic and human life by creating eutrophication, mutagenic, carcinogenic effects and dysfunction of the organs [2].

Dyes are classified to non-ionic-disperse, acid and reactive, cationic-basic and anionic direct dyes. the biggest and the most diverse group among synthetic dyes are constituted by Azo dyes containing one or more azo groups (-N=N-). Methylene blue's (MB)

name is 3,7-bis (dimethylamino)-phenothiazine-5-ium chloride. It is a fully synthetic chemical and was first used in the treatment of malaria [3,4]. In many applications which are related to medicine such as biomedical dyes applicable in cell staining, cancer phototherapy, antidepressant agents, cyanide, antimicrobial chemotherapy and poisoning by carbon oxide, Alzheimer's disease treatment by methemoglobinemia, MB has been studied among others, since the first report in 1876 [5].

In the structure of the MB, the presence of the electrons which are delocalized from the joined p-bonds (chromophore group) is the main cause for its blue color at the times when it is in aqueous solution and it is also responsible for the red color that it has in toluene which has the same mole amount of hydroxide. Due to MB's clear color, it can be applied as a dye and also for paper industry and staining in the textile [6-7].

Synthetic dyes can be lost at the time of manufacturing or it may be disposed to the environment among industrial wastewaters. The amount of its loss is estimated to be ca. 30% [8]. Considering MB's oral LD50 of 3500 mg kg^{-1} (in mice), it is not considered as a compound that is highly hazardous [9].

However, using doses of MB that are higher than 7.0 mg kg^{-1} can make abdominal pain and vomiting. It can also cause blood pressure to go high or nausea and mental disorder and other problems. Reports of chronic exposure to MB have indicated that it is mutagenic and causes reproductive disorder [10].

World health organization (WHO) prescribes a limit of 1mg L^{-1} of coloring substances in drinking water [11]. Therefore, there is an urgent need for appropriate and functional devices in order to remove MB from wastewaters.

For removing dyes from effluents of industry, some biological and physical or chemical methods have been used such as flocculation, coagulation, precipitation, adsorption on activated carbon, filtration of the membrane, biosorption, electrochemical methods, oxidation/ozonation and anaerobic/aerobic treatments. Various techniques of dye removing from wastewaters have some advantages and disadvantages [12]. Adsorption method was the only one considered to be best and superior among many other physicochemical methods which have been tested. Some of the advantages of this method in comparison with others are as follows: low-cost requirement, easily available, simple design, biodegradability, ease of

operation, high efficiency and also the ability to treat dyes in forms that are more concentrated [13-15].

The principle of treatment using adsorption method is dyes entrapment by a solid compound. Generally, according to the various studies conducted by scientists, activated carbon is a good adsorbent element for treatment of discoloration but it makes high-cost problems and saturates quickly and after being used it should be removed [16]. Then the research is lead to use adsorbents with low cost like agricultural wastes, these are very abundant in nature and effective and functional for dyes adsorption from aqueous solutions.

In recent years, different low cost biosorbents like date stones [17], Wheat straw [18], Arthrospira platensis [19], Sunflower seed hull [20], Penicillium YW 01 [21], Burkholderia vietnamiensis C09V [22], Bacillus catenulatus JB-022 strain [23], Saccharomyces cerevisiae spent [24], Symphoricarpus albus [25], Shrimp shell [26], and Algal spirogyra sp. [27], have been utilized for dyes removing from aqueous solutions.

The adsorption capacities of dyes by different natural adsorbent have been extensively reviewed by Lakayan *et al*. [28]. For example, the adsorption percentage for methylene blue was 98.5 % into walnut sawdust coated with polypyrrole (PPy). Ansari *et al*. have synthesized PPy/SD for adsorption of methylene blue from aqueous solution [29]. Kholghi *et al*. successfully used Azolla A. Filiculodes species for bio-sorption of Acid Red 14 (AR14) dye (64.5%) from aqueous solution [30]. Asfaram *et al*. reported an adsorption capacity of 37.96 mgg^{-1} for Direct Red 12B removal using Garlic Peel [31].

In this paper, Spruce sawdust (SD) as an agricultural waste, low-cost adsorbent and eco-friendly has been explored as the adsorbent for removing the MB in the batch system from aqueous solution.

Using materials like zinc oxide and magnesium oxide nanoparticles as a powerful sorbent on the surface of other adsorbents (e.g. AC) has a lot of advantages [32, 33]. The increase in the sorption active sites numbers onto the adsorbent can be caused by this process. The problems relevant to the separation of nanoparticles from the solution can also be solved by this process [32]. In this investigation, in order to enhance SD's capacity for the adsorption of MB dye, magnesium oxide nanoparticles (MgO) were fixed onto SD.

158

J. Water Environ. Nanotechnol., 3(2): 157-172 Spring 2018

For empirical design, creating an experimental model and also analyzing the models that are built and using a group of numerical and statistical methods is needed and therefore the Response Surface Methodology (RSM) is applied. RSM is based on a polynomial equation fitting to the experimental data, in order to describe the relationship between the response of interest and several variables with the objective of the effects evaluation of independent variables, their interaction effects, and also obtaining optimum conditions for the desirable responses [34].

Box-Behnken design (BBD) is usually utilized by the RSM. It was propounded by Box and Wilson [35]. The aim of using such a design is to diminish the number of experiments for the particular optimization process. Moreover, it also makes this opportunity for the chemist to investigating the effects of inter-variable that would not be possible with one traditional variable in a time technique. Therefore, BBD is a meticulous method to design the experiment and also to avoid the data redundancy [36]. Analysis of variance (ANOVA) is a statistical technique that is widely employed to assess the significance of various variables into the adsorption process.

Investigating the condition which is optimum for maximum adsorption of MB dye on synthesized Spruce sawdust coated with Magnesium oxide nanoparticles (SD/MgO) was the objective of this study. The BBD model was used for precisely figuring out the role of individual process parameters and also optimization of process variables. Moreover, synthesized SD/MgO nano-biocomposite was characterized by using FTIR, FE-SEM, XRD, and BET in order to determine desirable modification.

MATERIALS AND METHODS
Chemicals and materials

Sawdust samples (SD) were prepared from Spruce wood (Pterocarpus indicus) and were obtained from a local carpentry workshop (north of Iran). In order to remove the adhering dirt and foreign particles, the SD was washed first. The SD which was cleaned, dried using the light of the sun but the oven was made dry by keeping it at 60 °C in one night. The dried materials were crushed and then sieved through 180 μm mesh size.

MB is a dye having the empirical formula $C_{16}H_{18}N_3S$, λ (665nm) and a molecular mass M=319.86 g Mol⁻¹; the molecular structure is represented in Fig. 1. This organic dye is applied to examine the adsorption capacity of adsorbent. By dissolving of 0.5 g of dye in 1 liter of distilled water, a stock solution was made, and dilution was done due to gain the demanded concentrations [37]. Methylene blue dyes utilize in this study was provided by Samchun Chemicals Ltd.

A trans instruments pH meter (model HP3040) with a combined double junction glass electrode was used for measuring pH. All the grade chemicals needed for analysis were from Merck (Germany) and Sigma– Aldrich Chemical Co. (USA).

Preparation and modification of the adsorbent

In a chemical modification, 5.0 g SD with the given characteristics (180 μm mesh size, 10% humidity) was treated with 0.3M Magnesium sulfate heptahydrate ($MgSO_4.7H_2O$) and then, NaOH was added dropwise to the mixture under stirring at room temperature until the precipitation was completed. Then the modified SD was washed with double distilled water and filtered. The modified SD were dried in an oven at 90 °C for 6 h [38]. The desired absorbent means nanoparticles MgO coated on SD was prepared (Fig. 2 a). This heating causes the conversion of magnesium hydroxide deposits formed by the reaction to magnesium oxide.

$$Mg^{2+} + 2\,OH^- \rightarrow Mg(OH)_2(s) \tag{1}$$

$$Mg(OH)_2(s) \xrightarrow{\Delta} MgO(s) + H_2O \tag{2}$$
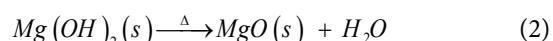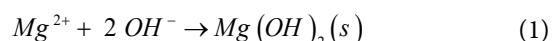
Characterization of adsorbent

The surface images the adsorbents of was captured before adsorption process by applying a Mira 3-XMU (TESCAN, Czech Republic) field emission scanning electron microscope (FE-SEM).

The surface functional groups of adsorbent were analyzed by FTIR spectroscopy (Agilent, Cary 630 2017). The spectra were recorded from 600 to 4000 cm⁻¹ with a number of scans 45.

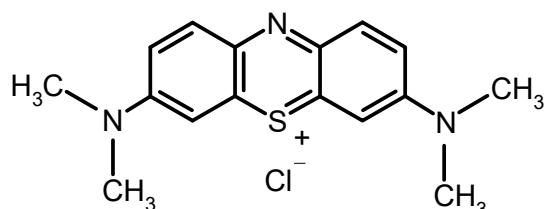The patterns of powder X-ray diffraction (XRD) were recorded in step scanning on a Philips

Fig. 1: Molecular structure of Methylene blue.

J. Water Environ. Nanotechnol., 3(2): 157-172 Spring 2018

159

PW3050 X-ray diffractometer by applying Cu Kα radiation (k=1.5406 Å) operating at 40 kV and 40 mA. XRD patterns were recorded in the range of 0–70° (2θ).

Nitrogen adsorption-desorption measurement was carried out on a BELSORP-max analyzer (BEL, JAPAN) at –196 ^{O}C after the sample was degassed at 120 ^{O}C in an N$_2$ flow.

Adsorption studies

The removal of MB dye was carried out by batch adsorption process. It was done under these effects: optimized adsorbent's amount, concentration and time and RSM which was based on BBD were adopted for this task.

The initial pH of dye solutions was adjusted using 0.1 N NaOH and 0.1 N HCl. The MB dye contents before and after adsorption processes were analyzed by UV/VIS spectrophotometer (Cary- Eclipse). The results obtained after equilibrium was reached, were fitted to various adsorption isotherms.

Equilibrium experiments were accomplished by putting some measured amount of sawdust in 250-mL flasks which contained 100 mL of dye solution of various initial amounts of dye (50–160 mg L^{-1}). The mixture was vibrated in an orbital shaker at 150 rpm while maintaining a constant temperature (25 ^{O}C). The solid phase was then separated by centrifugation (6000 rpm) through the liquid. Then, the dye concentration was measured at 664 nm maximum methylene blue wavelength using a UV-visible spectrophotometer. The adsorption isotherm models which are used more frequently than others were used in the present research and they are Freundlich [39], the Langmuir [40], Redlich–Peterson [41] and Temkin [42].

Kinetics experiments were done in 250 mL flasks which contain 100 mL of the dye solutions applying a 0.35 g of SD/MgO nano-biocomposite. The flasks were agitated for various time intervals (30–300 min) on the orbital shaker at 150 rpm while the temperature remained constant (25 ^{O}C). The kinetic data was analyzed using pseudo-first order, pseudo-second order [43] and intraparticle diffusion [44] and elovich kinetic models [45].

The picture of dye solution before and after the adsorption process for removing the MB dye by using SD/MgO nano-biocomposite is given in Fig. 3.
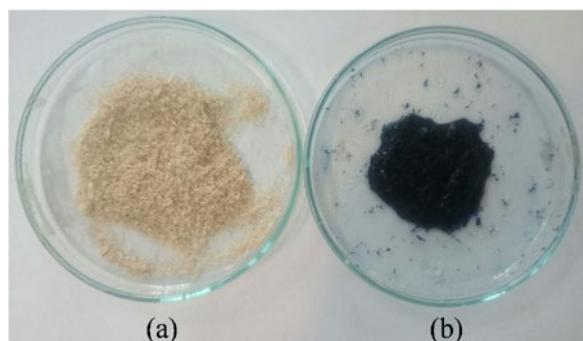

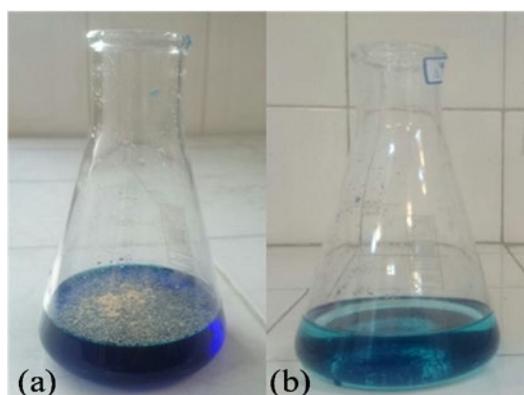Fig. 2: Photographs of SD/MgO powder (a) and SD/MgO-loaded MB (b).

Fig 3: Picture of dye solution before (a) and after (b) the adsorption process using SD/MgO.

160

J. Water Environ. Nanotechnol., 3(2): 157-172 Spring 2018

In order to get values from the samples, the measurement from all of the samples was taken in triplicates and then the mean values were calculated and were used for further analysis. The following equations were used to determine the capacity of the equilibrium adsorption and dye removal%:

$$q_e = (C_o - C_e) \times \frac{V}{M} \qquad (3)$$

$$Dye\ Re\,moval\,(\%) = \left(\frac{C_o - C_e}{C_o}\right) \times 100 \qquad (4)$$

q_e (mg g^{-1}) represents the capacity of the equilibrium adsorption while C_o and C_e are the initial and equilibrium dye concentrations (mg L^{-1}), respectively. V is the volume of the dye solution (L) and W is the dry weight of the adsorbent (g).

Box–Behnken design

BBD presents some advantages of other RSM like full factorial and central designs of composite due to its fewest points of design. Also, BBD offered treatment combinations at the edge's midpoint and the center of the process. But then, BBD avoidance of the experimental points which are extreme (corner and star points) led to a more efficient estimation of the coefficients. [46-47]. In this research, three factors with three BBD levels were applied to study the effects of variables; MB concentration, adsorbent dosage, and pH on the response factor; on removing of MB. The three levels of each variable; low, middle and high were encoded as −1, 0 and 1, respectively as in Table 1. 15 designed experimental BBD run with the independent variable arrangement; three response factors have been displayed in Table 2. Three responses of the central point were considered to estimate the pure error.

To correlate the MB removal, a quadratic polynomial equation was developed as a function of independent variables and their interactions. The correlation's general form is as follows:

$$Y = \beta_0 + \sum_{i=1}^{k} \beta_i X_i + \sum_{i=1}^{k} \beta_{ii} X_i^2 + \sum_{i=1}^{k}\sum_{i \prec j}^{k} \beta_{ij} X_i X_j + \varepsilon \qquad (5)$$

Y stands for the response factor (i.e., the removing of MB), X is input variable and β0, βj, βjj, βij are the intercept, the linear effect, the square effect, and the interaction effect, respectively. K is the quantity of input variables (3 in the current study) and ε is the unanticipated error [47]. The analyzing and optimization procedures and all the tables and figures were implemented using the Design-Expert 7.06 trial (Stat Ease, Inc. Minneapolis, USA).

RESULTS AND DISCUSSION
Characterization of nanobiocomposite SD/MgO Textural Properties

The physical properties of SD and SD/MgO nano-biocomposite samples were analyzed by low-temperature N$_2$ adsorption-desorption and the results are listed in Table 2. According to Table 1, the SD/MgO nano-biocomposite exhibits a high total surface area (0.873 m^2 g^{-1}) and lower pore diameter (6.858 nm). The results demonstrate that the presence of MgO nanoparticles enhances the total surface area and decreases the pore diameter.

Field Emission Scanning Electron Microscopy (FE-SEM)

Scanning Electron Microscopy is one of the most widely employed technique to obtain the information regarding the surface and morphology of the nanomaterials. The morphological information of the SD/MgO nano-biocomposite was obtained by FE-SEM.

Table 1: Experimental range and factor level of process variables applied in the experimental design.

Independent variables	Coded variables	Range and levels		
		Low (−1)	Middle (0)	High (+1)
MB concentration (mg L^{-1})	X$_1$	50	100	150
adsorbent dosage (g L^{-1})	X$_2$	1.5	2.5	3.5
pH	X$_3$	3	7	11

Table 2: Physical properties of the SD and SD/MgO nano-biocomposites.

Sample no	Total Surface area (m^2 g^{-1})	pore diameter (nm)	micropore surface area (m^2 g^{-1})	external surface area (m^2 g^{-1})
SD	0.455	14.653	0.205	0.250
SD/MgO	0.873	6.858	0.238	0.635

J. Water Environ. Nanotechnol., 3(2): 157-172 Spring 2018

161

The FE-SEM images of the SD and SD/MgO nano biocomposite are represented in Fig. 4. It is evident that sawdust is a smooth and layered material without any pores (Fig. 4a). This structure would account for its weak BET surface area. In contrast, the surface of the chemically modified sawdust has a large amount of MgO particles within the range of 40-60 nm (Fig. 4b).

Moreover, it also represents that most of the particles are quite homogeneous, have spherical-like shapes and are distributed on the SD surface, uniformly. This is obvious that the present material has high surface area and is therefore capable of adsorption of objective constituents.
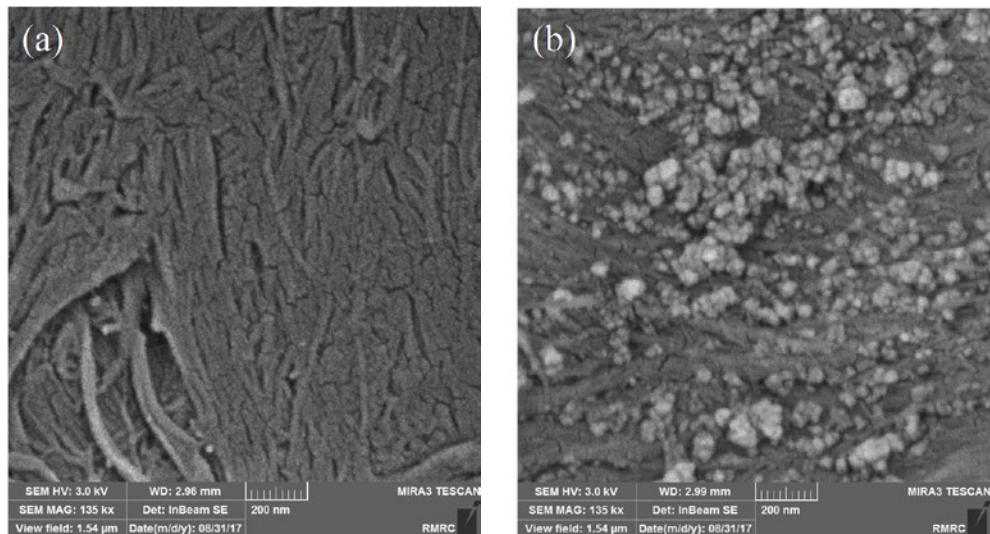
X-ray diffraction studies

XRD analysis obtained from SD and SD/MgO nano-biocomposite samples (Fig. 5) reveals that both adsorbents are completely amorphous. However, peaks emerge at $2\theta = 26, 38, 50, 59, 64$ and 69, suggesting the appearance of MgO crystals in SD/MgO [48].

The crystallite sizes (nm) were calculated by the Scherrer equation [49]. The mean nanocrystal size of the prepared SD/MgO has estimated about 5.2 nm. using the Debye-Scherrer formula on the basis of the full width at half maximum (FWHM) of the $2\theta = 38^{\circ}$ peak.

Fig: 4. FE-SEM micrographs for (a) untreated Spruce sawdust (SD) and (b) SD/MgO
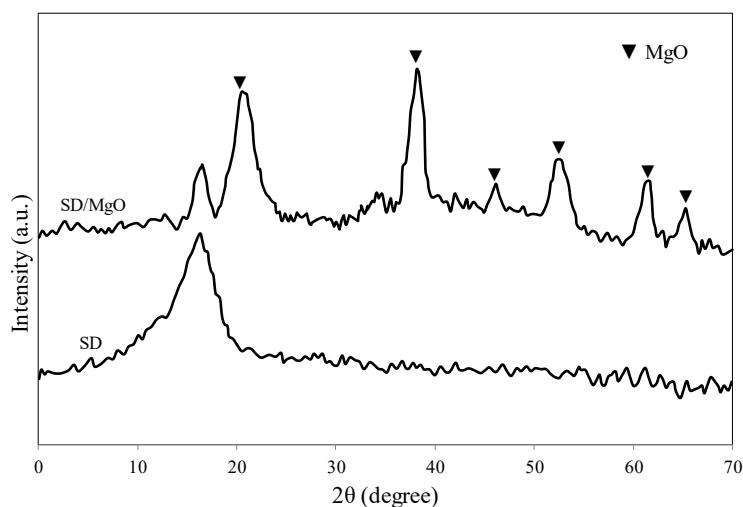
Fig. 5: XRD diffractogram of the SD and SD/MgO nano biocomposites.

162

J. Water Environ. Nanotechnol., 3(2): 157-172 Spring 2018

FTIR studies

The various groups present in adsorbent which are the potential sites to bin dye ion on the adsorbent surface are detected by the FTIR spectroscopy technique.

The spectra of SD/MgO before adsorption of MB and after that were analyzed within the amounts between 600-4000 cm^{-1} (Fig. 6). The FTIR spectrum of SD/MgO before MB adsorption displayed a number of peaks at various wavenumbers retaining to different functional groups. The appearance of the O-H group (phenols, carboxylic acids, and alcohols) on the adsorbent's surface as it happens in cellulose has been indicated by the presence of broad bands in the region of 3300 cm^{-1}, pectin and lignin [50,51].

The peak's presence in the area of 2900 cm^{-1} attributed to aliphatic C-H asymmetric stretching present in present in biomass structure (cellulose, hemicellulose, lignin) [50,52]. The peak at 1735 cm^{-1} is a correspondence to C=O stretching vibration of carboxylic acids groups [53,54]. C=C aromatic stretching of lignin assigns the bands in the region 1595 cm^{-1} and 1504 cm^{-1} to itself [55].

The bands at 1230 cm^{-1} and 1025 cm^{-1} corresponds to C-O stretching vibration of carboxylic acids and alcohols [-56, -57]. The bending vibration of C-H can cause the band at 896 cm^{-1} [-58]. After adsorption of MB, we note that the peaks intensity of O-H (3300 cm^{-1}), C=O (1735 cm^{-1}) and C-O (1230 cm^{-1}, 1025 cm^{-1}) decreased, these shifts indicate that an interaction occurred between MB and these groups. These results showed that the SD/MgO nanocomposite contains several functional groups responsible for the MB adsorption such as O-H, C=O, and C-O. Some new peaks have been detected on the SD/MgO spectrum after adsorption at 1330 and 1247 cm^{-1} for aromatic nitro compound and S=O stretching, respectively, attributed to the MB molecules presence on the surface of adsorbent [59].

Statistical analysis

Three factors with three levels of Box–Behnken response surface design (BBD) have been applied to investigate the dependent variables' features. These factors were used to optimize and study the process variables' effect on the response (MB Removing). The variables design matrix of not coded and coded units by the BBD; along with the values of the response which are experimental and predicted, is presented in Table 3. Each experiment was carried out three times and the average results of the MB Removal evaluation over the SD/MgO nano-biocomposites and their corresponding standard deviation values were reported. After that, the values of their related standard deviation were given. By reviewing the following table data, it is clear that the range of the values related to the deviation of the results was between 0.0 and 0.3 %, thus they were relatively low. Moreover, the values related to the relative standard deviation of the results were about ±2.3% and therefore they also were low, which approves that the experiments have good accuracy and reproducibility.

The values of MB removal which are measured in different batches presented wide variation (i.e., the range of values was from a minimum of 31.20
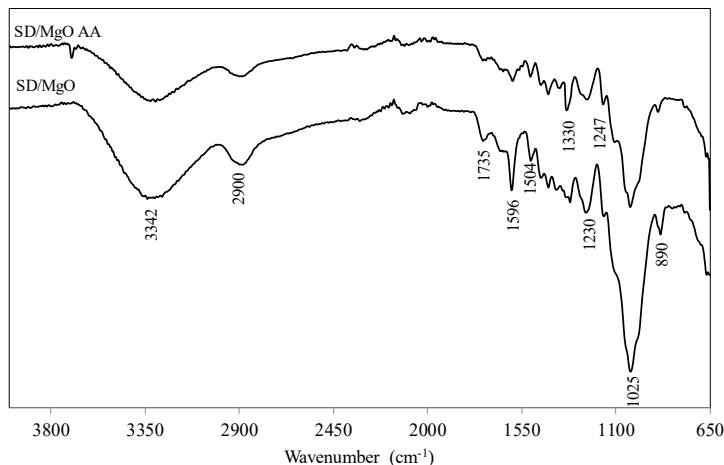

Fig. 6: The FTIR spectrums of SD/MgO before and after adsorption (SD/MgO AA) of MB.

J. Water Environ. Nanotechnol., 3(2): 157-172 Spring 2018

163

to a maximum of 93.36). The fact that the value of MB removal is highly affected by the variables selected for the study is clearly shown in the results.

A quadratic model with statistical significance from a combination of estimates for the variables and the ANOVA results can be produced. This model is given below:

$$MB \ Re moval\% = 55.61393 - 0.84416X_1 + 28.42542X_2 - 1.28880X_3 + 1.39417 \times 10^{-3}X_1^2$$
$$- 2.97958X_2^2 + 0.30799X_3^2 + 0.08625X_1X_2 + $$
$$0.013575X_1X_3 - 0.64625X_2X_3$$

(6)

Here, MB removal is the response and X_1, X_2 and X_3 are the actual parameters. The coefficient's sign and value in each correlation' term show the effects

of the parameters on the response increasing and decreasing.

From eq. (6) it can be concluded that the dosage of the adsorbent which has the coefficient of 28.42542, has the most positive linear impact among other ones and the interaction that is between the concentration of MB and the dosage of adsorbent which has a coefficient of 0.08625 has the most positive interaction impact on the removal of MB.

Table 4 shows the results of ANOVA test. It also shows the parameters which are based on statistics and are related to the suggested correlation which are quadratic. The F-Value (its other name is F-statistic) of a factor is something that is used to measure the assessment of the variance which

Table 3: Design matrix for experimental factors and response at different factor levels.

Experiment order	Experimental factors			Response (MB Removal)	
	MB concentration (mg L⁻¹)	Adsorbent dosage (g L⁻¹)	pH	Actual	Predicted
1	150 (+1)	2.50 (0)	11 (+1)	71.23	72.86
2	50 (-1)	3.50 (+1)	7 (0)	88.00	89.96
3	50 (-1)	2.50 (0)	3 (-1)	77.84	76.21
4	150 (+1)	2.50 (0)	3 (-1)	45.25	45.31
5	100 (0)	2.50 (0)	7 (0)	62.98	63.41
6	100 (0)	2.50 (0)	7 (0)	63.70	63.41
7	100 (0)	2.50 (0)	7 (0)	63.54	63.41
8	150 (+1)	1.50 (-1)	7 (0)	31.20	29.23
9	50 (-1)	2.50 (0)	11 (+1)	92.96	92.90
10	100 (0)	3.50 (+1)	3 (-1)	74.84	74.51
11	100 (0)	3.50 (+1)	11 (+1)	93.36	91.46
12	100 (0)	1.50 (-1)	3 (-1)	32.18	34.08
13	100 (0)	1.50 (-1)	11 (+1)	61.04	61.37
14	150 (+1)	3.50 (+1)	7 (0)	72.85	73.12
15	50 (-1)	1.50 (-1)	7 (0)	63.60	63.33

Table 4: Analysis of variance (ANOVA) for the response surface quadratic model.

Source	Sum of squares	Degree of freedom	Mean square	F value	p-Value Prob > F
Model	5065.93	9	562.88	134.58	< 0.0001
X_1	1297.19	1	1297.19	310.14	< 0.0001
X_2	2486.18	1	2486.18	594.41	< 0.0001
X_3	978.59	1	978.59	233.97	< 0.0001
$X_1 . X_2$	74.39	1	74.39	17.79	0.0083
$X_1 . X_3$	29.48	1	29.48	7.05	0.0451
$X_2 . X_3$	26.73	1	26.73	6.39	0.0527
X_1^2	44.85	1	44.85	10.72	0.0221
X_2^2	32.78	1	32.78	7.84	0.0380
X_3^2	89.67	1	89.67	21.44	0.0057
Residual	20.91	5	4.18		
Lack of fit	20.63	3	6.88	48.10	0.0204
Pure error	0.29	2	0.14		
Cor Total	5086.84	14			

is related to that factor and the residual variance. This value is calculated by dividing the mean square of the factor by the residual mean square. In most cases, in order to realize the configuration of interactions among the variables as the criteria, the ''Significance probability'' (its other name is ''p-value'') and F-statistic can be applied. The corresponding variables being more significant is shown by a higher F-statistic and a lower P-value and if the factor with P-value is lower than 0.05, it is regarded as significant.

As Table 4 shows, all quadratic and linear terms are below 0.05 and therefore significant except the interaction term of 'X$_2$X$_3$'. Nonetheless, because of the p-value ($p < 0.0001$) and F-statistic (F = 134.58), it can be concluded that this model is highly significant and it also approves the curvature' presence in the surface of the response.

The determination's coefficient of the proposed correlation is shown in Table 5. The definition of coefficient of variation (C.V) explains the standard deviation which is related to the mean and is also a statistical measure of dispersion.

Table 4 helps us approve that the regression model can portray the empirical data with a satisfying level of assurance (which is higher than 95%) by indicating that the low value of the coefficient of variation is 3.08% and the high value for determination coefficient is 0.9959 and adjusted determination coefficient is 0.9885.

Fig. 7 illustrates the empirical data points on the MB's removal. These data points are also compared with the values that are predicted. The quantified response data which are for a specific run are actual values. The approximating functions were used to generate the predicted values which are evaluated from the model. Fig. 7 also proves that the empirical results have a fine agreement when they are compared to the values that are predicted.

Effect of process variables on MB removal

Fig. 8 displays the plots of the mean effect which are based on the data from Table 4. When there is a response which is as large as possible in these experiments, it is concluded that the system is optimized. It is observable that adsorbent dosage

and pH have a positive impact on the MB removal and MB concentration has the negative impact. As the Table 4 shows, the adsorbent dosage is the highest effective degree of the individual factor on MB removal (F = 594.41, $p < 0.0001$).

In the case of adsorbent dosage, a clear increment in MB removal is seen by making the adsorbent dosage go from 1.5 to 3.5 g L^{-1}. Furthermore, the MB removal was decreased by increasing the MB concentration. Considering the pH, MB removal was enhanced by increasing this factor. At the low level of X$_1$ and high level of X$_2$ with increasing pH to the upper level, MB removing went higher.

Effect of experimental parameters on MB removal

3D response surface plots for the measured responses have been constructed in order to reach the better understanding of the independent variables effects and their interactions on the dependent variable. When a circular 3D response of the surfaces was found, the interaction between the related variables was negligible. Moreover, the plot's elliptical or saddle characters proves that the interaction between the related variables was significant [60].

Furthermore, parallel lines propose that no significant interaction has existed. In 3D response plots, the dependent variable is represented by the
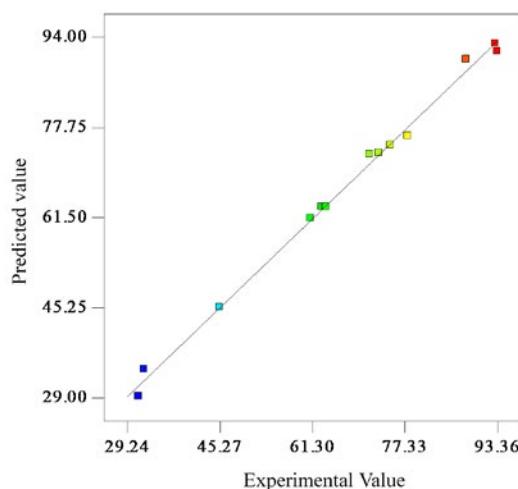

Fig. 7: Predicted vs. experimental values for removal of MB.

Table 5: Summary of the main statistical specifications of the response surface quadratic correlation.

Std. dev.	2.05	R-squared	0.9959
Coefficient of variation (C.V. %)	3.08	Adjusted R-squared	0.9885
Adequate precision	38.124	Predicted R-squared	0.9350

J. Water Environ. Nanotechnol., 3(2): 157-172 Spring 2018

165

upper horizontal axis. Illustrating the response surfaces as three dimensional (3D) plots determined the importance of each three independent factors (MB concentration, adsorbent dosage, and pH) on the removal of MB. Three-dimensional plots for MB removal were obtained from Eq. (6) and given in Fig. 9.

Fig. 9 (a) showed 3D response surface plots for percentage removal of MB on SD/MgO nano biocomposite as a function of MB concentration

and pH. In this removal percentage of MB increased with increasing pH of the solution (from pH 3 to 11). Curve portion in 3D plot Fig. 9 (a) suggested that significant removal of MB was found to have the almost good interactive influence of these two variables.

The percentage removal of dye increases with increase in an adsorbent dose of the solution. Curve portion in 3D plot Fig. 9 (b) suggested that significance removal of MB dye was found almost
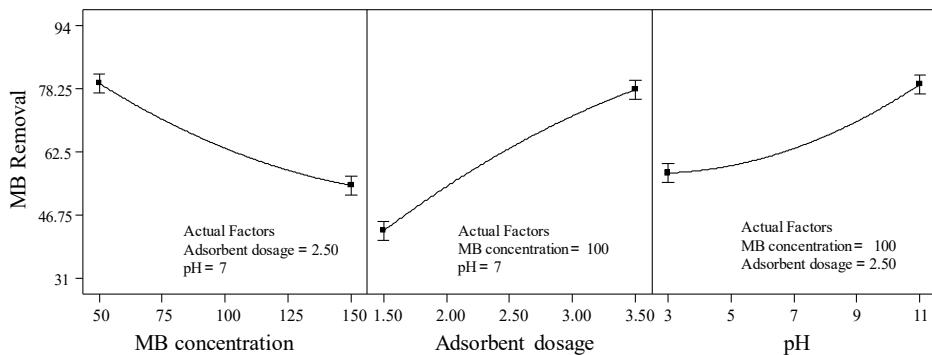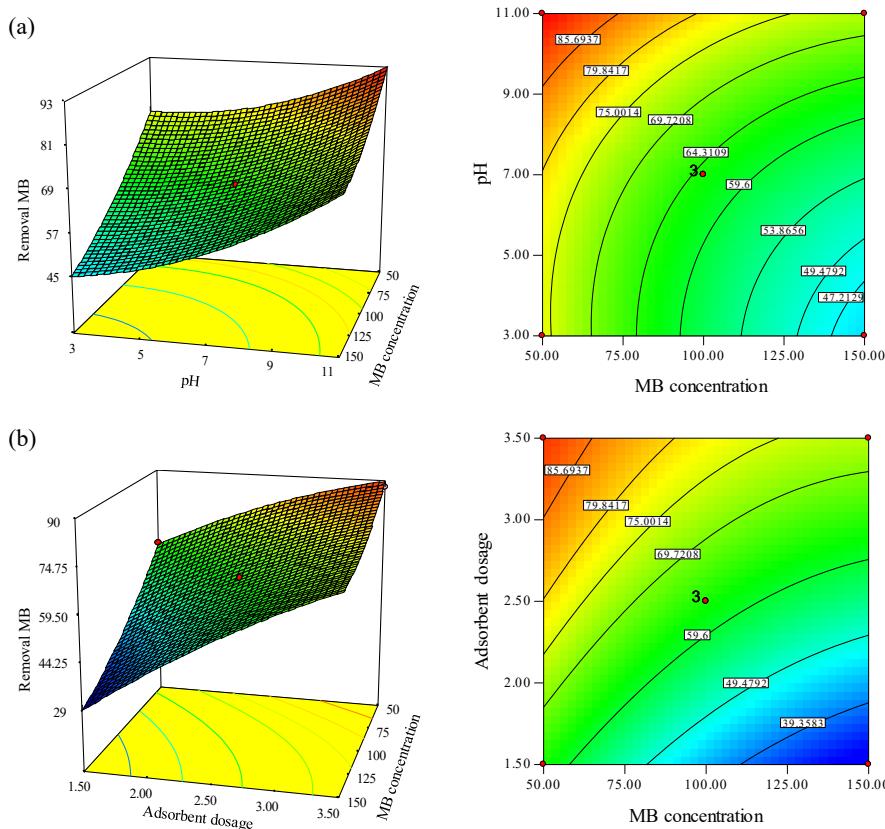

Fig. 8: Main effects of each variable on MB removal.

(a)

(b)

Fig. 9: Contours and response surface plots for MB removal as a function of (a) MB concentration vs. pH at adsorbent dosage=2.50 g L⁻¹ (b) MB concentration vs. adsorbent dosage at pH=7.

166

J. Water Environ. Nanotechnol., 3(2): 157-172 Spring 2018

good interactive influence as the adsorbent dose was increased from 1.50 to 3.5 g L^{-1}. At low doses (1.50 g L^{-1}), because of the limited number of binding sites that are available, there is less opportunity among dye molecules, therefore removal process attained a low percentage. Because of the more adsorption sites which are available for dye uptake, an increase in adsorbent dose to 0.20 g L^{-1}, would cause a corresponding increase in the percentage of removal [-61].

The F values for MB concentration, adsorbent dosage, and pH are 310.14, 594.41 and 233.97 according to Table 4, which affirms that adsorbent dosage has the highest important impact on MB removal.

Model validation for MB dye

The validation experiment was performed by several sets of different combination of variables (MB concentration, adsorbent dosage, and pH) each within their experimental ranges. The model predicted value, and the experimental value was used to define the validity of model (Table 6). These results affirm that the predicted conclusions satisfactorily match with the empirical values adequately.

On the basis of the best-fitted equation, the model optimization of variables was done to get the maximum removal percentage. 12 optimized results were obtained and it was found that the maximum optimized conditions for MB dye (MB concentration of 68.54 g L^{-1}, the dose of adsorbent 3.45 g L^{-1} and pH 10.48) which showed 94.05% removal of MB.

Kinetic study

In wastewater treatment, it is of great import to study the adsorption mechanism and steps of the potential rate controlling for design objectives. To describe the kinetics of adsorption, several kinetic models are available. Mostly applied models including the pseudo-first-order, pseudo-second-order, Elovich and intra-particle diffusion have been used for the empirical data to evaluate the adsorption kinetic of MB dye. The applicability of these kinetic models was appointed by measuring the correlation coefficients (R^2).

Pseudo-first and second-order kinetics

Below the pseudo-first-order and pseudo-second-order kinetic models' nonlinear equations are showed:

Table 6: Comparing the experimental and predicted values.

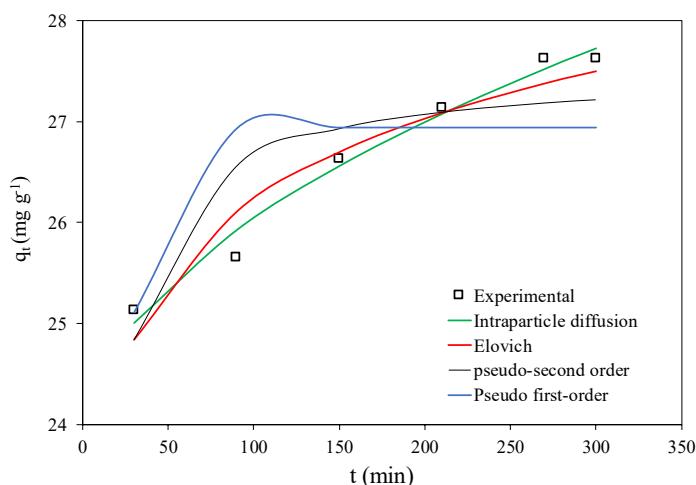| Run no.	MB concentration (mg L^{-1})	adsorbent dosage (g L^{-1})	pH	MB removal	
				Experimental [a]	Predicted
1	60	1.75	5	60.75±0.045	59.33
2	120	2.30	8	59.61±0.026	58.35
3	75	2.80	6	72.65±0.087	73.09
4	140	3.25	10	81.09±0.054	80.82

[a] Mean ± standard deviation.

Fig. 10: The analysis of the various kinetic models for the adsorption of MB on SD/MgO at 298K (C_o: 100 mg L^{-1}) by the non-linear method.

J. Water Environ. Nanotechnol., 3(2): 157-172 Spring 2018

167

$$q_t = q_e(1 - e^{-k_1 t})$$ (7)

$$q_t = \frac{k_2 q_e^2 t}{1 + k_2 q_e t}$$ (8)

k_1 stands for the pseudo-first-order rate constant (min^{-1}) and k_2 stands for the pseudo-second-order rate constant (g mg^{-1} min^{-1}). The MB' amount which is adsorbed at equilibrium is represented by q_e (mg g^{-1}). q_t (mg g^{-1}) stands for the MB's amount that is adsorbed at time t. Fig. 10 shows the graph of log (q_e - q_t) against 't' from which the pseudo-first-order kinetic rate constant was obtained.

The Fig. 10 shows the pseudo-second-order kinetic model. As can be seen in Table 7 a better R^2 value was obtained (R^2-0.875). The q_e values which were obtained were highly in support of the data from the research experiments for the related kinetic model. The involvement of chemical adsorption process is suggested by the applicability of the pseudo-second-order kinetic equation.

Elovich model

The reactions that include the adsorption of chemicals and also Elovich model can be employed easily. In order to analyze the range of chemisorption, this can be an important model to use. Below is the mathematical representation of the model:

$$q_t = \frac{1}{b}\ln(ab) + \frac{1}{b}\ln t$$ (9)

"a" is a constant. Because (q_t/t) equals "a" at the time that the value of q_t reaches 0, "a" is considered

Table 7: Parameters of the kinetic models for MB adsorption by SD/MgO with non-linear method (C_0 = 100 mg L^{-1}, adsorbent mass = 3.5 g L^{-1}, pH = 11, time = 30-300 min and T = 25 ^{o}C).

Models	Parameters	Values
	K_1	26.94452
First order	q_e (calc)	0.08963
kinetic model	q_e (exp)	27.6285
	R^2	0.5027
	K_2	0.01123
Second order	q_e (calc)	27.51291
kinetic model	q_e (exp)	27.6285
	R^2	0.875
	a	71498463
Elovich	b	0.865
	R^2	0.9321
Intraparticle	K_{id}	0.22984
diffusion	C	23.74767
	R^2	0.977

as the initial rate constant (mg g^{-1} min^{-1}). "b" (g mg^{-1}) represents the facade coverage's level and activation energy. q_t (mg g^{-1}) represents the MB's adsorption onto SD/MgO sorbent at time t. Plotting q_t against t evaluates the constants. Fig. 10 points out the fact that MB dye and SD/MgO nano biocomposite is following this model very well (see Table 7).

Intra-particle diffusion model

An intra-particle diffusion model was applied to investigate the kinetics of adsorption for MB dye and SD/MgO nano-biocomposite system. Below is the mathematical representation of this model:

$$q_t = k_{id} t^{0.5} + C$$ (10)

k_{id} stands for the intra-particle diffusion (mg g^{-1}) rate constant. C stands for the intercept (mg g^{-1}) and its value shows the boundary layer's thickness. Different parameters are being yielded from the plots of q_t versus t which describe that the process of batch adsorption involves more than one process. Furthermore, the Fig. 10 proposes that the intra-particle diffusion can be accepted as rate controlling step. The kinetic parameters and coefficients of the correlation are being shown in Table 7.

Equilibrium adsorption isotherm studies

The equilibrium isotherms are of great import elements for grasping the adsorption systems [62]. Different models (e.i. Langmuir, Freundlich, Temkin, and Redlich–Peterson) have been selected in order to simulate the adsorption isotherm and therefore clarify interactions of dye adsorbent.

Langmuir isotherm model

Langmuir isotherm model is studied for the surface which is covered by adsorbate monolayer. Langmuir isotherm describes the surface coverage of adsorbate monolayer (MB). Below is the mathematical representation of the nonlinear form of this model:

$$q_e = \frac{q_o K_L C_e}{1 + K_L C_e}$$ (11)

q_o represents the maximum amount of the capacity of adsorption (mg g^{-1}) and q_e stands for the amount of analyte which is adsorbed per unit mass of the adsorbent at equilibrium condition (mg g^{-1}). The values of respective constants of Langmuir are given in Table 8 and the graph plotted between q_e

168

J. Water Environ. Nanotechnol., 3(2): 157-172 Spring 2018

Table 8. Parameters related to Isotherms models for MB adsorption by SD/MgO with non-linear method (C_o = 50-160 mg L^{-1}, adsorbent mass = 3.5 g L^{-1}, pH = 11, time = 180 min and T = 25 °C).

Models	Parameters	Values
Langmuir	K_L	0.31525
	q_o	56.60
	R^2	0.9651
Freundlich	K_F	16.27124
	n	2.24
	R^2	0.9848
Temkin	K	3.8666
	B	11.51
	R^2	0.9537
Redlich–Peterson	A	87.33
	g	0.6135
	B	4.48
	R^2	0.9836

and C_e as shown in Fig. 12.

The suitability of the model is estimated by separation parameter (R_L) that can be evaluated by the following equation.

$$R_L = \frac{1}{1 + K_L C_o} \tag{12}$$

The R_L values were plotted against C_o to estimate the favourability of the adsorption of the process with respect to the initial concentration of the dye (Fig. 11). The fact that the nature of the isotherm is favorable ($0 < R_L < 1$), reversible ($R_L = 0$), linear ($R_L = 1$) or unfavorable ($R_L > 1$) is indicated by the values of the parameters of the separation. Value of R_L in this study was in the between of 0–1 which reveals that adsorption of MB onto SD/MgO nano-biocomposite was a favorable process. For this system, the R_L values approach towards zero as the initial concentration is increased.

Freundlich isotherm model

The isotherm model assumes heterogeneity in the adsorbent' surface which arises cause of the fact that there are different functional groups at the adsorbent's surface. Mathematically, a nonlinear form of this model is represented as.

$$q_e = K_F C_e^{1/n} \tag{13}$$

where K_F and n are Freundlich constants which represent Freundlich adsorption capacity (mg g^{-1}) and its intensity. The values of respective constants of Freundlich are given in Table 8. The Freundlich isotherm is shown in Fig. 12.

Temkin isotherm

Temkin isotherm is applied to survey the adsorption heat and indirect effect of the adsorbate interactions on adsorption. The model portrays the correlation of coverage with the adsorption energy and it takes no notice of the concentrations that are extreme. To Plot the amount of adsorbed q_e against C_e concluded that the homogenous spreading of binding energies was done. Below is the nonlinear form of Temkin isotherm:

$$q_e = B \ln(KC_e) \tag{14}$$

B = RT/b and T represents the absolute temperature (Kelvin), b stands for the Temkin constant and R represents the universal gas constant (8.314 J mol^{-1} K^{-1}). A stand for the constant of the equilibrium binding and B represents the related heat of sorption. Table 8 presents the findings' summary from the isotherm studies. If the experimental data fits better to the Temkin isotherm model, the high value of R^2 (0.9537) will be achieved.
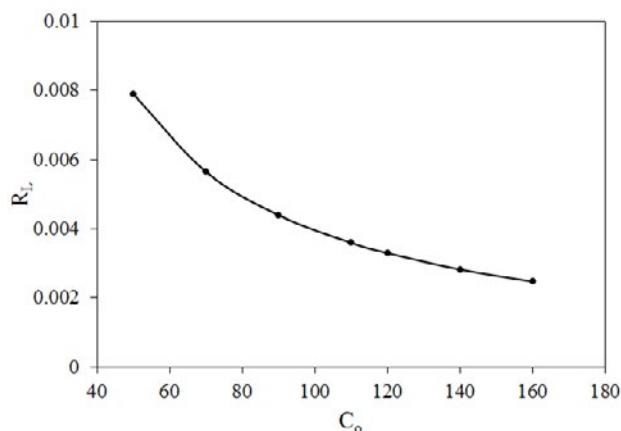

Fig. 11: Variation in R_L with respect to C_o of adsorption of MB.
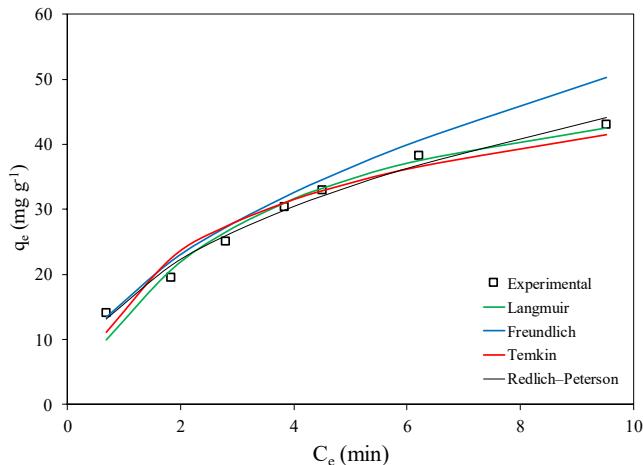
J. Water Environ. Nanotechnol., 3(2): 157-172 Spring 2018

169

Fig. 12: Isotherms obtained using the non-linear method for the adsorption of MB on SD/MgO.

Redlich–Peterson isotherm model Redlich–Peterson equation included three adjustable parameters into an empirical isotherm. This equation is widely used as a compromise between Langmuir and Freundlich systems. The nonlinear form of Redlich–Peterson isotherm model is represented as.

$$q_e = \frac{A\,C_e}{1 + B\,C_e^{\,g}} \qquad (15)$$

WhereA, B, and g are the Redlich–Peterson isotherm constants, q_e is the amount adsorbed at equilibrium (mg g^{-1}) and C_e is the equilibrium concentration of adsorbate (mg L^{-1}). When the value of g is equal to 1, the above equation is reduced to the Langmuir isotherm, while it reduced to a Freundlich isotherm, in case the value of the parameter $BC_e^{\,g}$ is much bigger than 1. The ratio of A/B indicates the adsorption capacity. The higher R^2 value (0.9846) for the three-parameter isotherms suggest the applicability of these models to represent the equilibrium adsorption of MB by SD/MgO nano-biocomposite. The values of the constants related to diverse isotherm models are presented in Table 8.

CONCLUSIONS

In this study, Spruce sawdust (SD) coated with MgO nanoparticles has been identified as effective adsorbent and this effective adsorbent is applied in a batch system for removing MB from aqueous solution. The synthesized SD/MgO nano-biocomposite was characterized by FTIR, FESEM, XRD, and BET. Further, RSM based BBD was carried out for optimization of variable parameters such as MB concentration, adsorbent dosage, and pH. R^2 0.9959 showed the significance of applied model for removal of MB dye. The model F-value of 134.58 and a low probability value (Prob. >F < 0.0001) signify that model terms are symbolic. Based on optimized conditions through RSM, maximum percentage removal of dye was found to be 94.05 % for MB. Moreover, validation of the model was done for dye removal to determine the correlation between experimental and predicted value. Resultant, a good percentage removal of dye was found on the basis of optimized methodology. The Freundlich isotherm model and pseudo-second-order kinetic model described the data better than other isotherm and kinetic models.

CONFLICT OF INTEREST

The authors declare that there are no conflicts of interest regarding the publication of this manuscript.

REFERENCES
1. Shukla, S.P., A. Singh, L. Dwivedi, K.J. Sharma, D.S. Bhargava, R. Shukla, N.B. Singh, V.P. Yadav, and Markandeya, 2014. Minimization of contact time for two-stage batch adsorber design using second-order kinetic model for adsorption of methylene blue (MB) on used tea leaves. International journal of scientific and innovative research, 2 (1): 58-66.
2. Abidi N, Errais E, Duplay J, Berez A, Jrad A, Schäfer G, et al. Treatment of dye-containing effluent by natural clay. Journal of Cleaner Production. 2015;86:432-40.
3. Pathania D, Sharma A, Siddiqi Z-M. Removal of congo red

dye from aqueous system using Phoenix dactylifera seeds. Journal of Molecular Liquids. 2016;219:359-67.

4. Gomes RF, de Azevedo ACN, Pereira AGB, Muniz EC, Fajardo AR, Rodrigues FHA. Fast dye removal from water by starch-based nanocomposites. Journal of Colloid and Interface Science. 2015;454:200-9.

5. Wainwright M, Crossley KB. Methylene Blue - a Therapeutic Dye for All Seasons? Journal of Chemotherapy. 2002;14(5):431-43.

6. Mills A, Hazafy D, Parkinson J, Tuttle T, Hutchings MG. Effect of alkali on methylene blue (C.I. Basic Blue 9) and other thiazine dyes. Dyes and Pigments. 2011;88(2):149-55.

7. Mohammadi, A. and A. Aliakbarzadeh Karimi, 2017. Methylene Blue Removal Using Surface-Modified TiO2 Nanoparticles: A Comparative Study on Adsorption and Photocatalytic Degradation, Journal of Water and Environmental Nanotechnology, 2(2): 118-128.

8. Essawy AA, Ali AE-H, Abdel-Mottaleb MSA. Application of novel copolymer-TiO2 membranes for some textile dyes adsorptive removal from aqueous solution and photocatalytic decolorization. Journal of Hazardous Materials. 2008;157(2-3):547-52.

9. Lewis, R.J., 1992. Sax's Dangerous Properties of Industrial Chemicals, eighth ed., Van Nostrand Reinhold, New York.

10. Oz M, Lorke DE, Hasan M, Petroianu GA. Cellular and molecular actions of Methylene Blue in the nervous system. Medicinal Research Reviews. 2010;31(1):93-117.

11. Sahu, R., 2015. Removal of Congo red dye from water using orange peel as an adsorbent, Thesis, National Institute of Technology, Rourkela – 769008, India.

12. Garg V. Basic dye (methylene blue) removal from simulated wastewater by adsorption using Indian Rosewood sawdust: a timber industry waste. Dyes and Pigments. 2004;63(3):243-50.

13. Sanghi R, Bhattacharya B. Review on decolorisation of aqueous dye solutions by low cost adsorbents. Coloration Technology. 2002;118(5):256-69.

14. Meshko V, Markovska L, Mincheva M, Rodrigues AE. Adsorption of basic dyes on granular acivated carbon and natural zeolite. Water Research. 2001;35(14):3357-66.

15. Toor M, Jin B. Adsorption characteristics, isotherm, kinetics, and diffusion of modified natural bentonite for removing diazo dye. Chemical Engineering Journal. 2012;187:79-88.

16. Ronda A, Martín-Lara MA, Almendros AI, Pérez A, Blázquez G. Comparison of two models for the biosorption of Pb(II) using untreated and chemically treated olive stone: Experimental design methodology and adaptive neural fuzzy inference system (ANFIS). Journal of the Taiwan Institute of Chemical Engineers. 2015;54:45-56.

17. El messaoudi, N., A. Lacherai, M. El khomri, S. Bentahar and A. Dbik, 2015. Modification of lignocellulosic biomass as agricultural waste for the biosorption of basic dye from aqueous solution, Journal of Materials and Environmental Science, 6: 2784–2794.

18. Zhao B, Shang Y, Xiao W, Dou C, Han R. Adsorption of Congo red from solution using cationic surfactant modified wheat straw in column model. Journal of Environmental Chemical Engineering. 2014;2(1):40-5.

19. Mitrogiannis D, Markou G, Çelekli A, Bozkurt H. Biosorption of methylene blue onto Arthrospira platensis biomass: Kinetic, equilibrium and thermodynamic

studies. Journal of Environmental Chemical Engineering. 2015;3(2):670-80.

20. Oguntimein GB. Biosorption of dye from textile wastewater effluent onto alkali treated dried sunflower seed hull and design of a batch adsorber. Journal of Environmental Chemical Engineering. 2015;3(4):2647-61.

21. Yang Y, Wang G, Wang B, Li Z, Jia X, Zhou Q, et al. Biosorption of Acid Black 172 and Congo Red from aqueous solution by nonviable Penicillium YW 01: Kinetic study, equilibrium isotherm and artificial neural network modeling. Bioresource Technology. 2011;102(2):828-34.

22. Cheng Y, Lin H, Chen Z, Megharaj M, Naidu R. Biodegradation of crystal violet using Burkholderia vietnamiensis C09V immobilized on PVA–sodium alginate–kaolin gel beads. Ecotoxicology and Environmental Safety. 2012;83:108-14.

23. Kim SY, Jin MR, Chung CH, Yun Y-S, Jahng KY, Yu K-Y. Biosorption of cationic basic dye and cadmium by the novel biosorbent Bacillus catenulatus JB-022 strain. Journal of Bioscience and Bioengineering. 2015;119(4):433-9.

24. El-Gendy NS, El-Salamony RA, Amr SSA, Nassar HN. Statistical optimization of Basic Blue 41 dye biosorption by Saccharomyces cerevisiae spent waste biomass and photo-catalytic regeneration using acid TiO2 hydrosol. Journal of Water Process Engineering. 2015;6:193-202.

25. Kara I, Akar ST, Akar T, Ozcan A. Dithiocarbamated Symphoricarpus albus as a potential biosorbent for a reactive dye. Chemical Engineering Journal. 2012;211-212:442-52.

26. Daneshvar E, Sohrabi MS, Kousha M, Bhatnagar A, Aliakbarian B, Converti A, et al. Shrimp shell as an efficient bioadsorbent for Acid Blue 25 dye removal from aqueous solution. Journal of the Taiwan Institute of Chemical Engineers. 2014;45(6):2926-34.

27. Khataee AR, Vafaei F, Jannatkhah M. Biosorption of three textile dyes from contaminated water by filamentous green algal Spirogyra sp.: Kinetic, isotherm and thermodynamic studies. International Biodeterioration & Biodegradation. 2013;83:33-40.

28. Lakayan, S., A. Baharlouei and E. Jalilnejad, 2016. Application of agricultural wastes as natural adsorbent for removal of industrial dyes, Journal of Studies in Color World, 6: 27-43.

29. Ansari R, Mosayebzadeh Z. Removal of basic dye methylene blue from aqueous solutions using sawdust and sawdust coated with polypyrrole. Journal of the Iranian Chemical Society. 2010;7(2):339-50.

30. Kholghi, S., Kh. Badii and S. H. Ahmad, 2013. Bio-Sorption Isotherm and Kinetic Study of Acid Red 14 from Aqueous Solution by Using Azolla A. Filiculodes, Journal of color science and technology, 6: 337-346.

31. Asfaram A, Fathi MR, Khodadoust S, Naraki M. Removal of Direct Red 12B by garlic peel as a cheap adsorbent: Kinetics, thermodynamic and equilibrium isotherms study of removal. Spectrochimica Acta Part A: Molecular and Biomolecular Spectroscopy. 2014;127:415-21.

32. Ghaedi M, Ghayedi M, Kokhdan SN, Sahraei R, Daneshfar A. Palladium, silver, and zinc oxide nanoparticles loaded on activated carbon as adsorbent for removal of bromophenol red from aqueous solution. Journal of Industrial and Engineering Chemistry. 2013;19(4):1209-17.

33. Changsuphan, A., M.I. Wahab and N.T. Kim Oanh, 2012.

J. Water Environ. Nanotechnol., 3(2): 157-172 Spring 2018

171

Removal of benzene by ZnO nanoparticles coated on porous adsorbents in presence of ozone and UV, Chemical Engineering Journal, 181: 215–221.

34. M.A. Bezerra et al., Response surface methodology (RSM) as a tool for optimization in analytical chemistry, Talanta 76 (2008) 965–977

35. Khodadoust S, Ghaedi M, Hadjmohammadi MR. Dispersive nano solid material-ultrasound assisted microextraction as a novel method for extraction and determination of bendiocarb and promecarb: Response surface methodology. Talanta. 2013;116:637-46.

36. Saad M, Tahir H, Khan J, Hameed U, Saud A. Synthesis of polyaniline nanoparticles and their application for the removal of Crystal Violet dye by ultrasonicated adsorption process based on Response Surface Methodology. Ultrasonics Sonochemistry. 2017;34:600-8.

37. Tsai W-T, Hsien K-J, Hsu H-C, Lin C-M, Lin K-Y, Chiu C-H. Utilization of ground eggshell waste as an adsorbent for the removal of dyes from aqueous solution. Bioresource Technology. 2008;99(6):1623-9.

38. Meshkani F, Rezaei M. Facile synthesis of nanocrystalline magnesium oxide with high surface area. Powder Technology. 2009;196(1):85-8.

39. Roosta M, Ghaedi M, Daneshfar A, Sahraei R. Experimental design based response surface methodology optimization of ultrasonic assisted adsorption of safaranin O by tin sulfide nanoparticle loaded on activated carbon. Spectrochimica Acta Part A: Molecular and Biomolecular Spectroscopy. 2014;122:223-31.

40. Kannusamy P, Sivalingam T. Synthesis of porous chitosan–polyaniline/ZnO hybrid composite and application for removal of reactive orange 16 dye. Colloids and Surfaces B: Biointerfaces. 2013;108:229-38.

41. Belhachemi M, Addoun F. Comparative adsorption isotherms and modeling of methylene blue onto activated carbons. Applied Water Science. 2011;1(3-4):111-7.

42. Acta Physicochimica U.R.S.S. Nature. 1935;136(3432):217-.

43. Temkin M.J. and V. Pyzhev 1940. Recent modifiications to Langmuir isotherms. Acta physicochimica URSS, 12: 217–22.

44. Srivastava V, Sharma YC, Sillanpää M. Response surface methodological approach for the optimization of adsorption process in the removal of Cr(VI) ions by Cu2(OH)2CO3 nanoparticles. Applied Surface Science. 2015;326:257-70.

45. Satapathy MK, Das P. Optimization of crystal violet dye removal using novel soil-silver nanocomposite as nanoadsorbent using response surface methodology. Journal of Environmental Chemical Engineering. 2014;2(1):708-14.

46. Lundstedt T, Seifert E, Abramo L, Thelin B, Nyström Å, Pettersen J, et al. Experimental design and optimization. Chemometrics and Intelligent Laboratory Systems. 1998;42(1-2):3-40.

47. Ferreira SLC, Bruns RE, Ferreira HS, Matos GD, David JM, Brandão GC, et al. Box-Behnken design: An alternative for the optimization of analytical methods. Analytica Chimica Acta. 2007;597(2):179-86.

48. Bakulina VM, Tokareva SA, Latysheva EI, Vol'nov II. X-ray diffraction study of magnesium superoxide Mg(O2)2.

Journal of Structural Chemistry. 1970;11(1):150-1.

49. Sharifi Pajaie H, Taghizadeh M. Optimization of nano-sized SAPO-34 synthesis in methanol-to-olefin reaction by response surface methodology. Journal of Industrial and Engineering Chemistry. 2015;24:59-70.

50. Ahmad A, Khatoon A, Mohd-Setapar S-H, Kumar R, Rafatullah M. Chemically oxidized pineapple fruit peel for the biosorption of heavy metals from aqueous solutions. Desalination and Water Treatment. 2015;57(14):6432-42.

51. Yagub MT, Sen TK, Afroze S, Ang HM. Fixed-bed dynamic column adsorption study of methylene blue (MB) onto pine cone. Desalination and Water Treatment. 2014;55(4):1026-39.

52. Pehlivan E, Tran HT, Ouédraogo WKI, Schmidt C, Zachmann D, Bahadir M. Sugarcane bagasse treated with hydrous ferric oxide as a potential adsorbent for the removal of As(V) from aqueous solutions. Food Chemistry. 2013;138(1):133-8.

53. Yu X, Tong S, Ge M, Wu L, Zuo J, Cao C, et al. Adsorption of heavy metal ions from aqueous solution by carboxylated cellulose nanocrystals. Journal of Environmental Sciences. 2013;25(5):933-43.

54. Oo CW, Kassim MJ, Pizzi A. Characterization and performance of Rhizophora apiculata mangrove polyflavonoid tannins in the adsorption of copper (II) and lead (II). Industrial Crops and Products. 2009;30(1):152-61.

55. Pavan FA, Lima EC, Dias SLP, Mazzocato AC. Methylene blue biosorption from aqueous solutions by yellow passion fruit waste. Journal of Hazardous Materials. 2008;150(3):703-12.

56. Feng N-c, Guo X-y. Characterization of adsorptive capacity and mechanisms on adsorption of copper, lead and zinc by modified orange peel. Transactions of Nonferrous Metals Society of China. 2012;22(5):1224-31.

57. Singh J, Ali A, Jaswal VS, Prakash V. Desalination of Cd2+ and Pb2+ from paint industrial wastewater by Aspergillus niger decomposed Citrus limetta peel powder. International Journal of Environmental Science and Technology. 2014;12(8):2523-32.

58. Deniz F, Kepekci RA. Dye biosorption onto pistachio by-product: A green environmental engineering approach. Journal of Molecular Liquids. 2016;219:194-200.

59. Nasuha N, Hameed BH, Din ATM. Rejected tea as a potential low-cost adsorbent for the removal of methylene blue. Journal of Hazardous Materials. 2010;175(1-3):126-32.

60. Doğar Ç, Gürses A, Açıkyıldız M, Özkan E. Thermodynamics and kinetic studies of biosorption of a basic dye from aqueous solution using green algae Ulothrix sp. Colloids and Surfaces B: Biointerfaces. 2010;76(1):279-85.

61. Ayed L, Achour S, Khelifi E, Cheref A, Bakhrouf A. Use of active consortia of constructed ternary bacterial cultures via mixture design for Congo Red decolorization enhancement. Chemical Engineering Journal. 2010;162(2):495-502.

62. Salleh MAM, Mahmoud DK, Karim WAWA, Idris A. Cationic and anionic dye adsorption by agricultural solid wastes: A comprehensive review. Desalination. 2011;280(1-3):1-13.

172

J. Water Environ. Nanotechnol., 3(2): 157-172 Spring 2018